Mass transport deposits in the Donegal Barra Fan and their association with British–Irish Ice Sheet dynamics

Srikumar Roy[1]*, Aggeliki Georgiopoulou[2], Sara Benetti[3] and Fabio Sacchetti[4]

[1]iCRAG, School of Earth Sciences, University College Dublin, Dublin D04 N2E5, Ireland

[2]School of Environment and Technology, University of Brighton, Cockcroft Building, Lewes Road, Brighton BN2 4GJ, UK

[3]School of Geography and Environmental Science, Ulster University, Cromore Road, Coleraine, BT52 1SA Northern Ireland, UK

[4]Marine Institute, Oranmore, Galway H91 R673, Ireland

AG, 0000-0003-4298-5090; SB, 0000-0001-6286-9842

*Correspondence: Srikumar.roy@icrag-centre.org

Abstract: This study analyses seismic data to investigate the kinematic indicators within the mass transport deposits (MTDs) of the Donegal Barra Fan complex in the Rockall Trough, along the NW European continental margin. Five episodes of mega-scale MTDs (DBF-01, -02, -03, -04 and -05) are identified. DBF-01 is the largest MTD in the NW British continental margin, comprising 1907 km^3 of sediments. Fold-and-thrusts were identified within the MTDs where they attain maximum thickness of *c.* 300–380 ms TWT, but not at the toe region. This indicates that local erosion and deceleration caused bulking up of the MTD volume, but the MTD was not fully arrested due to the high mobility of the mass flow. MTD thickness distribution and thrust fault orientations indicate source areas and flow direction of MTD. The MTDs show a compensational stacking pattern with earlier deposits influencing the position and flow direction of succeeding slides, suggesting that glaciogenic debris flows are sensitive to topographic variability. We propose that increased sediment input associated with at least five expansions of the British–Irish Ice Sheet to the shelf edge led to the development of these MTDs and that the youngest of them, DBF-05, corresponds to the Last Glacial Maximum.

Supplementary material: Seismic cross-section showing buttressing of DBF-02 and -03 against DBF-01 (Fig. 7c); thrusts within DBF-01 (Fig. 7c), DBF-04 overlying DBF-03 and its termination (Fig. 7c), DBF-05 buttressing against DBF-01, -02 and -03 (Fig. 3; refer to Fig. 5e for location) are available at https://doi.org/10.6084/m9.figshare.c.4816911

Submarine mass transport deposits (MTDs) involve upslope depletion and downslope accumulation of sediments along a basal shear surface, with the translated sediments often forming elevated topographic features on the contemporaneous seafloor (Varnes 1978). MTDs are a common occurrence on continental margins and are important in margin evolution. Bull *et al.* (2009) documented various types of kinematic indicators within MTDs including ramps-and-flats, fold-and-thrusts, which are of great importance to the understanding of the initiation, dynamic evolution, flow direction and cessation of MTDs (Frey-Martínez *et al.* 2005; Alsop *et al.* 2017).

MTDs constitute the bulk of sediments in trough mouth fans (TMFs) (Vorren and Laberg 1997). TMFs are stacks of glaciogenic debris flows forming prograding wedges on continental margins in front of palaeo-ice streams, which drained, among others, the former European Ice Sheets, the Greenland and West Antarctic Ice Sheets (Vorren and Laberg 1997; Stow *et al.* 2002; Rebesco *et al.* 2006; Dowdeswell *et al.* 2008). Hemipelagic or contouritic interglacial sediments often separate the glaciogenic debris flow units (Stow *et al.* 2002; Ó Cofaigh *et al.* 2003). TMFs of late Pliocene to Pleistocene age are recognized along the continental margin of NW Europe (Vorren and Laberg 1997; Dahlgren *et al.* 2005), and the southernmost of these is the Donegal Barra Fan (DBF) that was fed by the British–Irish Ice Sheet (BIIS) (Armishaw *et al.* 2000).

Two major MTD complexes have been identified in the Rockall Trough offshore Ireland: the Rockall Bank Slide Complex (RBSC) (Georgiopoulou *et al.* (2019) and references therein), and the DBF complex (Holmes *et al.* 1998; Armishaw *et al.* 2000; Knutz *et al.* 2002; Stow *et al.* 2002) (Fig. 1). The timing, failure mechanisms and number of slumping events of the RBSC have been studied

From: Georgiopoulou, A., Amy, L. A., Benetti, S., Chaytor, J. D., Clare, M. A., Gamboa, D., Haughton, P. D. W., Moernaut, J. and Mountjoy, J. J. (eds) 2020. *Subaqueous Mass Movements and their Consequences: Advances in Process Understanding, Monitoring and Hazard Assessments*. Geological Society, London, Special Publications, **500**, https://doi.org/10.1144/SP500-2019-177

using a wide variety of geophysical data and sedimentary cores (Flood *et al.* 1979; Georgiopoulou *et al.* 2013, 2019; Sacchetti *et al.* 2013), as well as simulation modelling studies of the major phases of slumping episodes during and before the Last Glacial Maximum (Salmanidou *et al.* 2018). However, we have a poor understanding of the various slumping events of the DBF complex, and their extent in the Irish sector of the Rockall Trough.

The objective of this study is to improve our understanding of the extent and dominant transport mechanisms of MTDs in the DBF complex by investigating the geometry, distribution, stacking patterns and kinematic indicators of individual MTDs, their interactions with the RBSC and potential links between MTDs and episodes of BIIS advances on to the NW European Irish continental shelf.

Geological setting

The NW European continental margin is characterized by a range of submarine features including TMFs deposited in front of fast-flowing ice streams, and MTDs formed by failure of accumulated glaciogenic and marine sediments and moraines (Dahlgren *et al.* 2005; Sejrup *et al.* 2005; Ó Cofaigh *et al.* 2012). A number of MTDs of various sizes and of Pliocene to Pleistocene age have been identified, including the

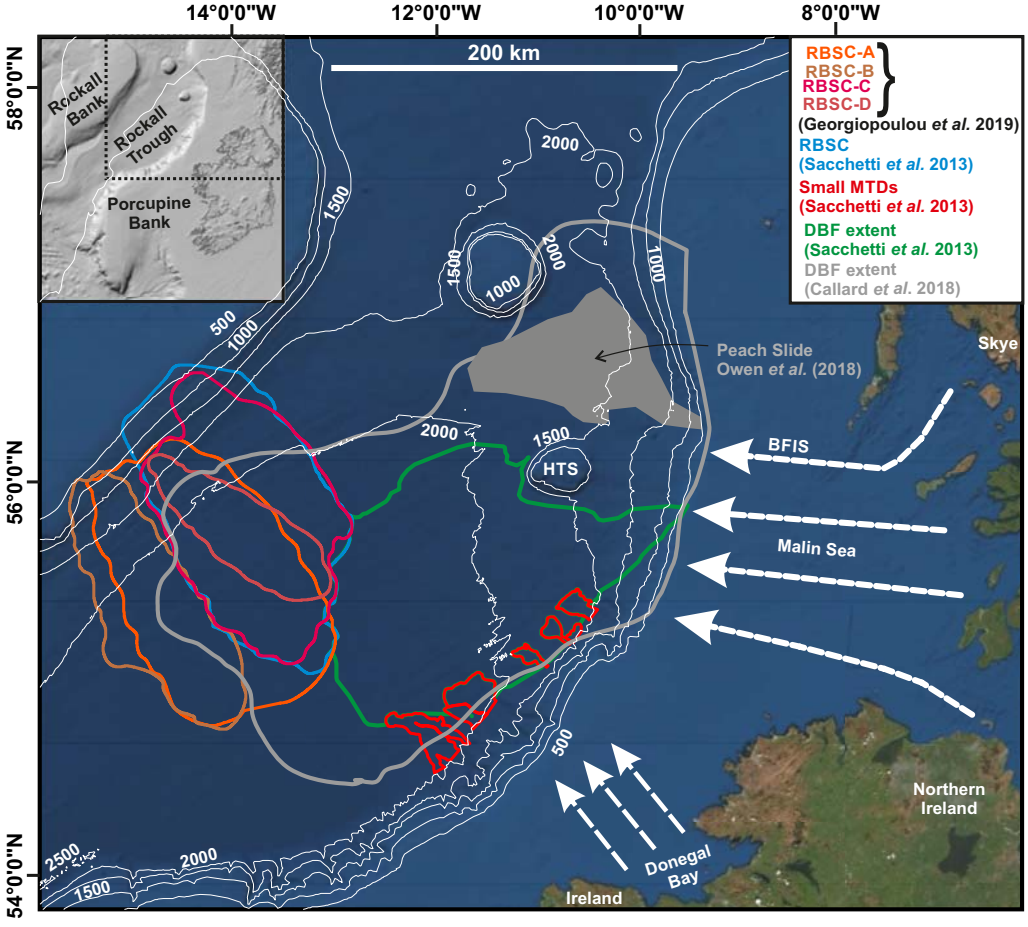

Fig. 1. Regional overview map of study area offshore Ireland showing key features: extent of Donegal Barra Fan (DBF), Rockall Bank Slide Complex (RBSC) and small MTDs (Sacchetti *et al.* 2013); four different slides of the RBSC (A, B, C and D) described by Georgiopoulou *et al.* (2019); DBF extent and location of the Barra Fan Ice Stream (BFIS) modified from Dunlop *et al.* (2010), Clark *et al.* (2012), Ó Cofaigh *et al.* (2012), Peters *et al.* (2016) and Callard *et al.* (2018). HTS, Hebrides Terrace Seamount. White arrows indicate general direction of ice flow. Basemap source: Esri, DigitalGlobe, GeoEye, CNES/Airbus, USDA, USGS, AeroGRID.

Storegga Slide Complex, the North Faroes Slide Complex and the Peach Slide (Haflidason *et al.* 2004; Evans *et al.* 2005; Sejrup *et al.* 2005; Owen *et al.* 2018). Most of the slides and debris flows on the continental slope north of 55° N are associated with glacial depocentres (Evans *et al.* 2005).

The Rockall Trough is the largest of the basins offshore west Ireland, with water depths ranging from 500 m on the eastern and western margins to almost 4000 m in the southern opening of the trough (Fig. 1). The Mid to Late Cenozoic stratigraphic framework for the Rockall Trough comprises three megasequences bounded by unconformities C30, C20 and C10 (Stoker *et al.* 2001). The C10 unconformity is an early Pliocene angular unconformity (*c.* 5 Ma) separating the early Miocene to early Pliocene megasequence from early Pliocene to Holocene sediments (McDonnell and Shannon 2001).

The seafloor and shallow sub-seafloor geomorphology of the deep-water Irish continental margin has been mapped in detail using a wide range of high-resolution geophysical datasets, revealing features such as submarine mass failures of various sizes and extent, escarpments, canyons and channels, sedimentary lobes associated with canyon systems, slab failures and evolved slides, incipient cuspate slides, etc. (Shannon *et al.* 2001; Unnithan *et al.* 2001; Elliott *et al.* 2010; Sacchetti *et al.* 2011, 2012, 2013; Georgiopoulou *et al.* 2013, 2014). Some of these features are the focus of this study and are discussed in more detail below.

The Donegal Barra Fan (DBF) and the British–Irish Ice Sheet (BIIS)

Reconstruction of the advance and retreat of the last BIIS on the continental shelf NW of Ireland is based on relatively recent geophysical and sedimentological datasets (Dunlop *et al.* 2010; Ó Cofaigh *et al.* 2012, 2019; Peters *et al.* 2016; Callard *et al.* 2018). Converging ice flows from NW Ireland and western Scotland merged on the Malin Sea Shelf in the Barra Fan Ice Stream (BFIS) (Fig. 1). The BFIS drained 5–10% of the BIIS (Dove *et al.* 2015) and fed sediments and meltwater towards the largest glacimarine depocentre of the BIIS, known as the DBF (Fig. 1). The BIIS reached the outer shelf and was grounded at the shelf break of the Malin Sea on more than one occasion (Fyfe *et al.* 1993). Bathymetric and sub-bottom data show that the ice was grounded extensively along the shelf edge in the Malin Sea Shelf and offshore of NW Ireland during the last offshore glacial advance (Benetti *et al.* 2010; Peters *et al.* 2015; Callard *et al.* 2018). Some ice streaming was also present in Donegal Bay (Greenwood and Clark 2009; Benetti *et al.* 2010; Ó Cofaigh *et al.* 2012), to the south of the Malin Sea, but the geophysical data on the continental margin do not show the development of a distinct TMF in this region (Sacchetti *et al.* 2012, 2013). The ice sheet reached its maximum extent at the shelf edge sometime before 26.5–26 ka BP (Clark *et al.* 2012; Peters *et al.* 2016; Callard *et al.* 2018). By 25.9 ka BP, the retreat of the BIIS from the shelf edge was already underway. The style of retreat was episodic and characterized by the formation of moraines and grounding zone wedges across the shelf (Dunlop *et al.* 2010; Callard *et al.* 2018; Ó Cofaigh *et al.* 2019). The outer continental shelf in the Malin Sea was free of grounded ice by 23.2 ka BP with the majority of the shelf ice-free by 19.5 ka BP (Callard *et al.* 2018). At this time, while the ice sheet was no longer grounded at the seafloor, it is likely that an ice shelf persisted in this region well into the deglacial period, with meltwater release and ice rafting occurring at least until 15.9 ka BP and resulting in episodes of downslope MTD on the DBF (Tarlati 2018).

The DBF covers an area of about 7000 km^2 and locally approaches 700 m in thickness in the deep-water basin of the Rockall Trough (Fig. 1; Owen and Long 2016). Armishaw *et al.* (2000) recognized a combination of different sedimentary processes dominant during the three-stage glacial to post-glacial evolution of this depositional system, which resulted in the composite nature of the DBF. The first and most significant sediment input was in the NE of the study area, where the DBF overlies the Late Miocene and Early Pliocene sediments and is distal in character. The sedimentary sequence comprises contourites, glaciomarine deposits and hemipelagic sediments (Armishaw *et al.* 2000). Continental uplift later contributed to the growth of the DBF during the mid-Pliocene; however, the majority of the DBF sediments were deposited during the Pleistocene when the fan was a major depocentre for the BIIS. The Peach Slide is the largest known MTD situated in the northern flank of the fan, consisting of four major debrite units (sediment volume *c.* 135–673 km^3), which were deposited during the period between 36.5 and 10.5 ka BP (Holmes *et al.* 1998; Knutz *et al.* 2001; Maslin *et al.* 2004). Shallow subsurface and surface geophysical imaging has allowed recent mapping and interpretation of contourites, hemipelagites and debrites within the Peach Slide (Owen *et al.* 2018).

Slides on the Rockall Trough margins

The RBSC is located along the western margin of the trough and to the east of the Rockall Bank (Fig. 1). It covers *c.* 18 000 km^2 of the base of slope and floor of the Rockall Trough (Elliott *et al.* 2010). Several studies have investigated high-resolution-bathymetry

data, GLORIA and TOBI side-scan sonar data, sub–bottom acoustic data, multichannel seismic data and sedimentary core data to study the morphology, multiple episodes of slumping and their ages (Shannon *et al.* 2001; Unnithan *et al.* 2001; Georgiopoulou *et al.* 2012, 2013; Sacchetti *et al.* 2013). The RBSC constitutes at least three voluminous episodes of slope collapse (sediment volume *c.* 125–400 km^3), a fourth less voluminous event, and possibly a fifth more localized event, which occurred during 200 to 22 ka (Georgiopoulou *et al.* 2019). The four larger MTDs are referred to as RBSC slides A, B, C and D in Georgiopoulou *et al.* (2019) and in this paper (Fig. 1).

Mass wasting on the western margin of the trough involved larger sediment volumes as compared to the relatively smaller slope failures of the eastern margin, where sediment was progressively evacuated towards the deeper basin through canyons (Georgiopoulou *et al.* 2014). In the northeastern Rockall Trough, a large mass transport complex was identified as the Erris Wedge in the buried sedimentary sequence directly overlying the C30 unconformity (Elliott *et al.* 2006). The Erris Wedge pinches out at the southern limit of the DBF.

Data and methods

The data used in this study include three surveys of 2D multichannel seismic data acquired over the past decades in offshore Ireland (Fig. 2). The most recent surveys, PAD-13 and PAD-14, were acquired by R/V *BGP Explorer* for ENI Ireland BV during 2013–14. The vessel was equipped with a Sercel G-Gun-II as a source, placed at a depth of 8 m (±1 m), and towed one streamer of length 10 050 m placed at 10 m (±1 m) depth. The survey was acquired with a shot-point interval of 37.5 m, 12 s record length, 2 ms sample rate and 50 ms recording delay. The unpublished PAD-13 and PAD-14 lines are of the best quality, spaced 40–50 km apart, and are the main dataset analysed for this paper. The

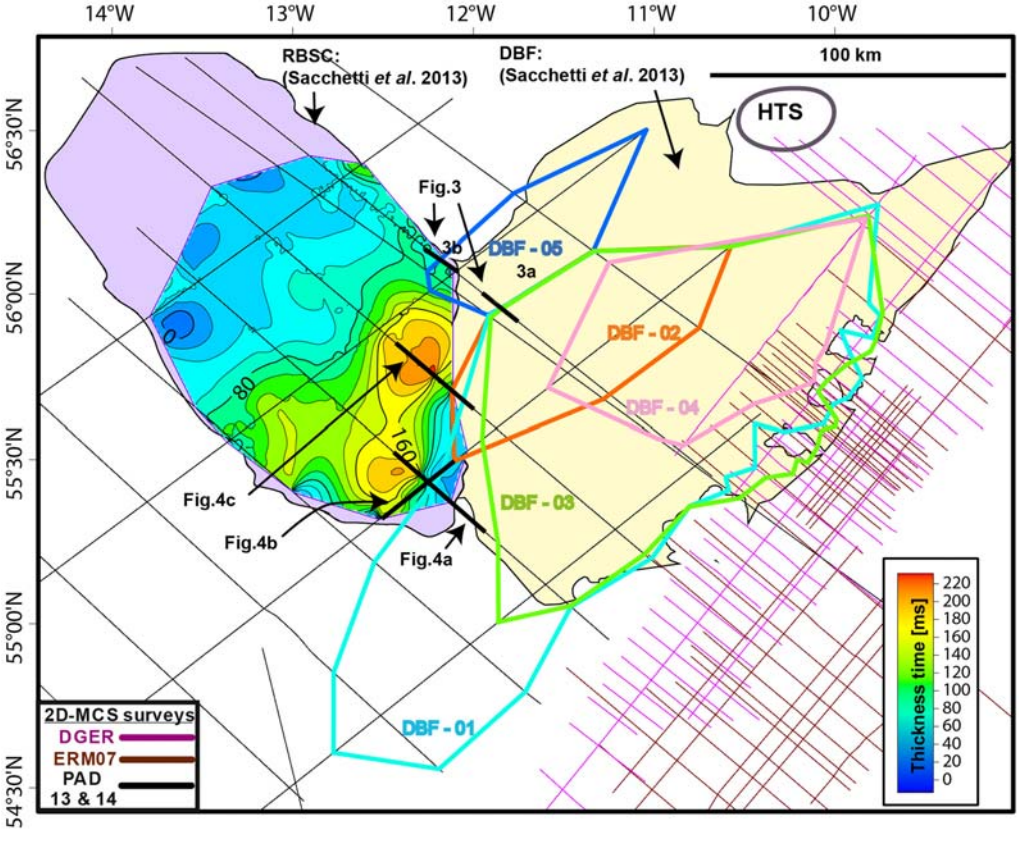

Fig. 2. Extent of previously published Rockall Bank Slide Complex (RBSC) and Donegal Barra Fan (DBF) complex (Sacchetti *et al.* 2013), along with the RBSC time thickness map (TWT, ms) calculated in this study, and the extent of different MTDs comprising the DBF complex in the northeastern part of the Irish Rockall Trough. HTS, Hebrides Terrace Seamount.

ERM07 2D seismic survey was acquired by M/V *Lazarev & Shatskiy* and M/V *Nalivkin* in 2007 for client TGS-Nopec Geophysical. The vessels used an airgun source placed at a depth of 7–10 m, and towed an 8090 m long streamer (648/636 channels) placed at a depth of 12 m. The survey was acquired using a shot-point interval of 25 m, group interval of 12.5 m and 9 s record length. The DGER 2D seismic survey was acquired by the M/V *Polar Princess* in 1996. The vessel used a source gun array (30 × 17.2 m) placed at a depth of 7 m, and towed a streamer 4500 m long placed at a depth of 8 m. The survey was acquired using CDP (common depth points) spacing of 6.25 m, shot-point interval of 25 m and 8 s record length. The above three sets of surveys were processed following standard industry procedure (Yilmaz 2001). The eastern slope of the Rockall Trough is covered by both the ERM07 and DGER surveys with an average spacing of 6–10 km between each seismic line. The ERM07 survey has good to moderate quality of seismic lines, especially in the shallow depths below the seafloor, whereas the DGER survey shows poor quality of seismic imaging in the shallow stratigraphic layers. The 50 km line spacing between the best quality PAD-13 and PAD-14 lines and closely spaced poor to medium quality DGER and ERM07 lines made the correlation of MTDs challenging in this study. All survey data have been made available by the Irish Petroleum Affairs Division (data available on request from https://www.dccae.gov.ie/en-ie/natural-resources/topics/Oil-Gas-Exploration-Production/data/regional-seismic-survey/Pages/Regional-Seismic-Survey.aspx).

The basal shear surface of each MTD, and deformation structures within the MTDs were interpreted in Petrel software, provided by Schlumberger. Thereafter, these surfaces were used to create isochron thickness maps, which were integrated with previously published geophysical interpretation using ArcGIS software for spatial correlation. The sediment volume of each of the MTDs was calculated by converting two-way time (TWT) into metres using an average P-wave velocity of 1700 m s^{-1} for less-consolidated marine sediments (Hamilton and Bachman 1982).

Results and discussion

This section presents and discusses the seismic interpretation of various MTDs that are part of the RBSC and the DBF (Figs 3–9).

RBSC

One of the MTDs within the RBSC has been mapped by Sacchetti *et al.* (2013) using shallow high-resolution geophysical datasets and corresponds with 'Slide C' of Georgiopoulou *et al.* (2019) (Figs 1 & 2). The termination of this MTD was mapped in the northwestern part of the study area. It shows a varied seismic character. The northern part of the MTD is characterized by a chaotic reflection pattern of low to moderate amplitudes (Fig. 3b). In contrast, the toe of the MTD at the southern end is characterized by moderate to high amplitude reflections, showing compressional features, such as reverse faults (Fig. 4a–c). The basal shear surface is typically a continuous, medium-high negative amplitude reflector, easily identified on the seismic data and is parallel to the slope stratigraphy (Figs 3b & 4).

Sediments show two main accumulations within the MTD. The thickness reaches up to 200 ms (TWT) in the southern portion of the MTD (Figs 2 & 4a), and 230 ms (TWT) 40 km north from the former location (Figs 2 & 4c). The volume of sediments calculated for the slide identified in this study is *c.* 660 km^3. The MTD identified as RBSC in this study ramps up a stratigraphic unit which is characterized by chaotic seismic facies (Fig. 4c). This chaotic seismic facies unit could be part of 'Slide A' identified by Georgiopoulou *et al.* (2019). This is observed only on one seismic line, and hence its extent could not be mapped.

DBF complex

After integrated data analysis with previously published results (Knutz *et al.* 2002; Sacchetti *et al.* 2013; Owen and Long 2016), all the MTD events interpreted in this study in the northeastern Rockall Trough were observed to lie above the C10 unconformity and beneath the RBSC, and hence are assumed to be part of the DBF complex. The MTD units have been recognized based on criteria established from previous studies (Evans *et al.* 1996; Frey-Martínez *et al.* 2005; Gamboa *et al.* 2011); each MTD unit was identified as a discrete stratigraphic unit covering a considerably large area, which is characterized internally by chaotic, semi-transparent, highly disrupted seismic facies distinctly different from the adjacent undeformed units and underlying stratigraphy. Detailed interpretation of five basal shear surfaces distinguished five separate MTDs within the DBF complex (Fig. 5). The basal shear surface for each MTD unit was identified in a similar way to unconformities, characterized by abrupt termination of a continuous medium-high amplitude reflection that dips parallel to the underlying chaotic seismic facies of the MTD units (Figs 3, 4, 6–9). Occasionally the basal shear surface is observed to ramp up or down the stratigraphy forming a step-like geometry (Fig. 8b, c). Most of the internal facies of the MTDs are chaotic and/or semi-transparent; however, occasionally, individual semi-continuous reflections within the MTD allow identification of internal facies and therefore better

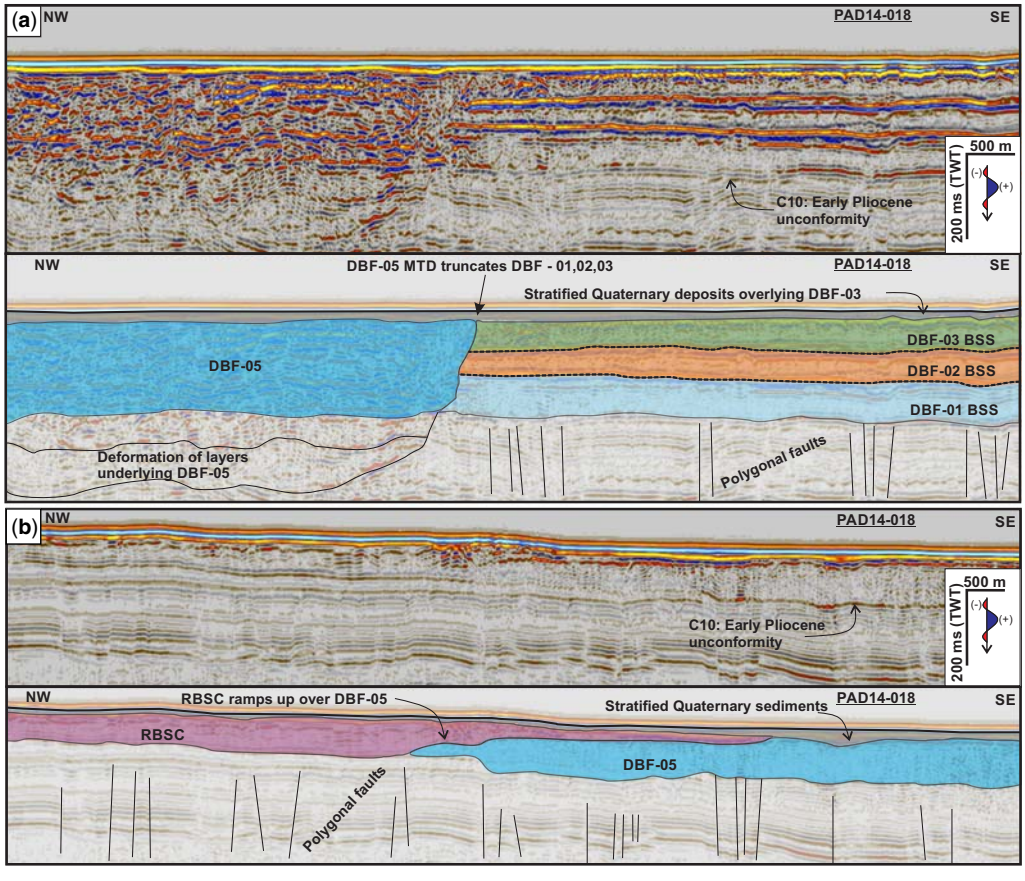

Fig. 3. (**a**) Seismic facies and basal shear zone of DBF-01, DBF-02, DBF-03 and DBF-05. Note the deformation of stratified layers beneath the DBF-05, and the buttressing nature of DBF-05 on DBF-01, DBF-02 and DBF-03. (**b**) RBSC ramps over DBF-05 in the NW Rockall Trough corner. Note thin veneer of stratified sediments (marked with grey colour) above MTDs. Refer to Figure 2 for location of seismic sections.

understanding of the internal architecture. The majority of these semi-continuous reflections are slightly tilted to the basal shear surface and the top of the MTDs. These features are interpreted as fold-and-thrust systems and described separately in the section on 'Flow processes within the DBF'. The areas and sediment volumes of each of the five MTDs interpreted in this study, comprising the DBF complex in the Irish sector of the Rockall Trough, are shown in Figure 10. They are further described below.

DBF-01

DBF-01 extends over the largest surface area out of the five identified MTDs. DBF-01 covers an area of *c.* 16 589 km^2 and consists of *c.* 1907 km^3 of sediments, making it the largest submarine MTD described along the NW British continental margin (Moscardelli and Wood 2016). It stretches over *c.* 258 km in length along a NE–SW direction and is *c.* 100 km wide in its central part. The present-day water depth varies from 1668 m in the NE to 2956 m in the SW over the extent of DBF-01. DBF-01 is not exposed to the seafloor. Almost 60% of DBF-01 is draped by succeeding MTDs (DBF-02, -03 and -04), which are all part of the DBF complex. In the southwestern region, stratified sediments drape *c.* 40% of DBF-01 (4790 km^2); these sediments could be either hemipelagic sediments, contourites or sediment gravity flows related to meltwater pulses. The stratified sediments are highly continuous and easily distinguished from the underlying chaotic seismic facies of the MTD (Fig. 4a, b). Two major depocentres have been identified in the central and southern part of DBF-01 (Fig. 5a). The thickness of these two depocentres varies from 300 to 350 ms (TWT) and are characterized by fold-and-thrust

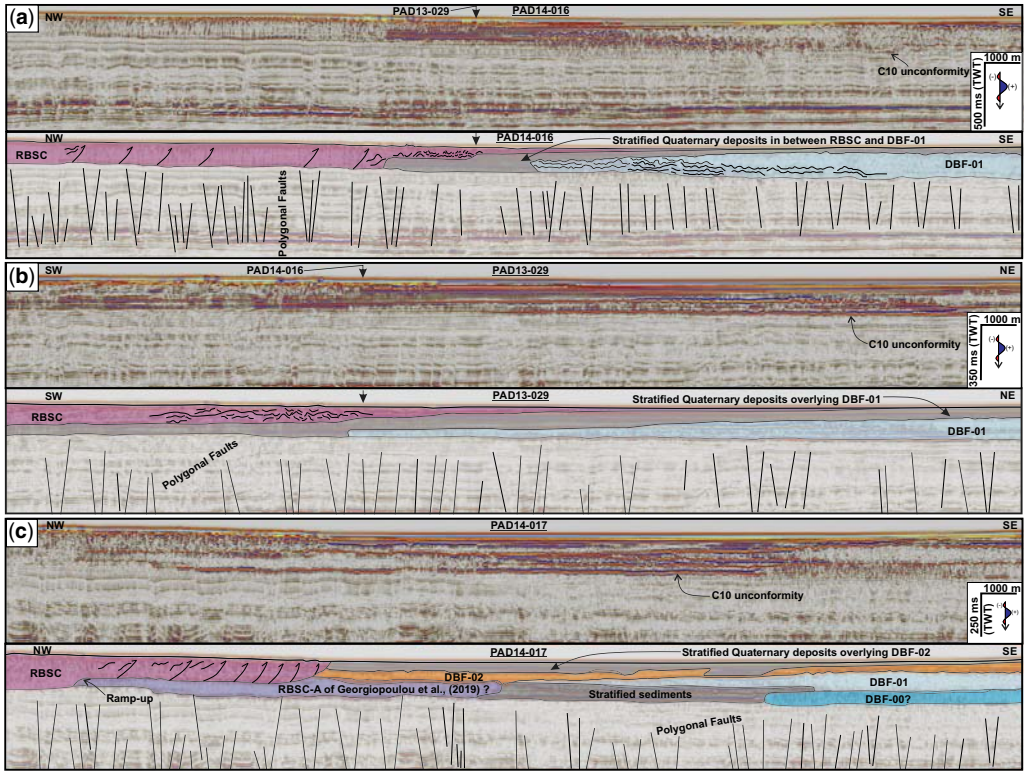

Fig. 4. (**a–c**) Compressional features within the RBSC toe section overlying stratified sediments and DBF-01and DBF-02 in the central and northern part of the Rockall Trough. Explanations of DBF-00 and RBSC-A have been given in text. Refer to Figure 2 for location of seismic sections.

systems (Figs 5 & 7). The orientation of individual thrusts is difficult to ascertain in this scenario, as we observe NW-verging thrusts on only one 2D seismic line, which is contradicted by a general NE–SW alignment of thickness map contour lines (Fig. 5a). However, we speculate that the thrusts might have formed due to the accumulation of downslope-translated sediments as part of a slope failure event. Sediments may have been brought in by the BFIS in the Malin Sea (NE–SW palaeoflow direction) and those derived by ice streaming in the Donegal Bay area (SE–NW palaeoflow direction) (Fig. 1; Clark *et al.* 2012).

Ten deformed rafted blocks, as defined by Frey-Martínez *et al.* (2005), have been identified within DBF-01. Nine of them are in the thicker northern part. One is located 63 km NE from the southern toe of the slide. The blocks are usually resting on the basal shear surface of the MTD (Figs 6b & 7a, b), but occasionally they are observed floating in the chaotic matrix of the MTD (Fig. 6c). The top of the rafted blocks are characterized by medium–high amplitude reflections and demonstrate different styles of internal deformation (minor, moderate and major) as classified in Gamboa *et al.* (2012). Irrespective of their location in relation to the main MTD mass, rafted blocks exhibit deformation with increasing translation or duration of sliding and tend to become aligned with their long axis parallel to the direction of flow (Huvenne *et al.* 2002; Bull *et al.* 2009). However, due to the coverage of the seismic data, we are unable to carry out detailed analysis of the spatial distribution of blocks or their internal character. A chaotic seismic unit underlying DBF-01 was identified on only one seismic line (Fig. 4c). This unit could possibly be part of the DBF complex and has been named DBF-00, but no further investigation was possible due to the limited seismic coverage.

DBF-02

This MTD is 115 km long, stretching along a NE–SW axis, and 45 km wide in the central part of the slide, draping the northwestern part of DBF-01 (Fig. 2). DBF-02 covers an area of *c.* 3653 km^2, draping *c.* 30% of DBF-01, and comprising *c.* 287 km^3 of sediments. It has the smallest volume

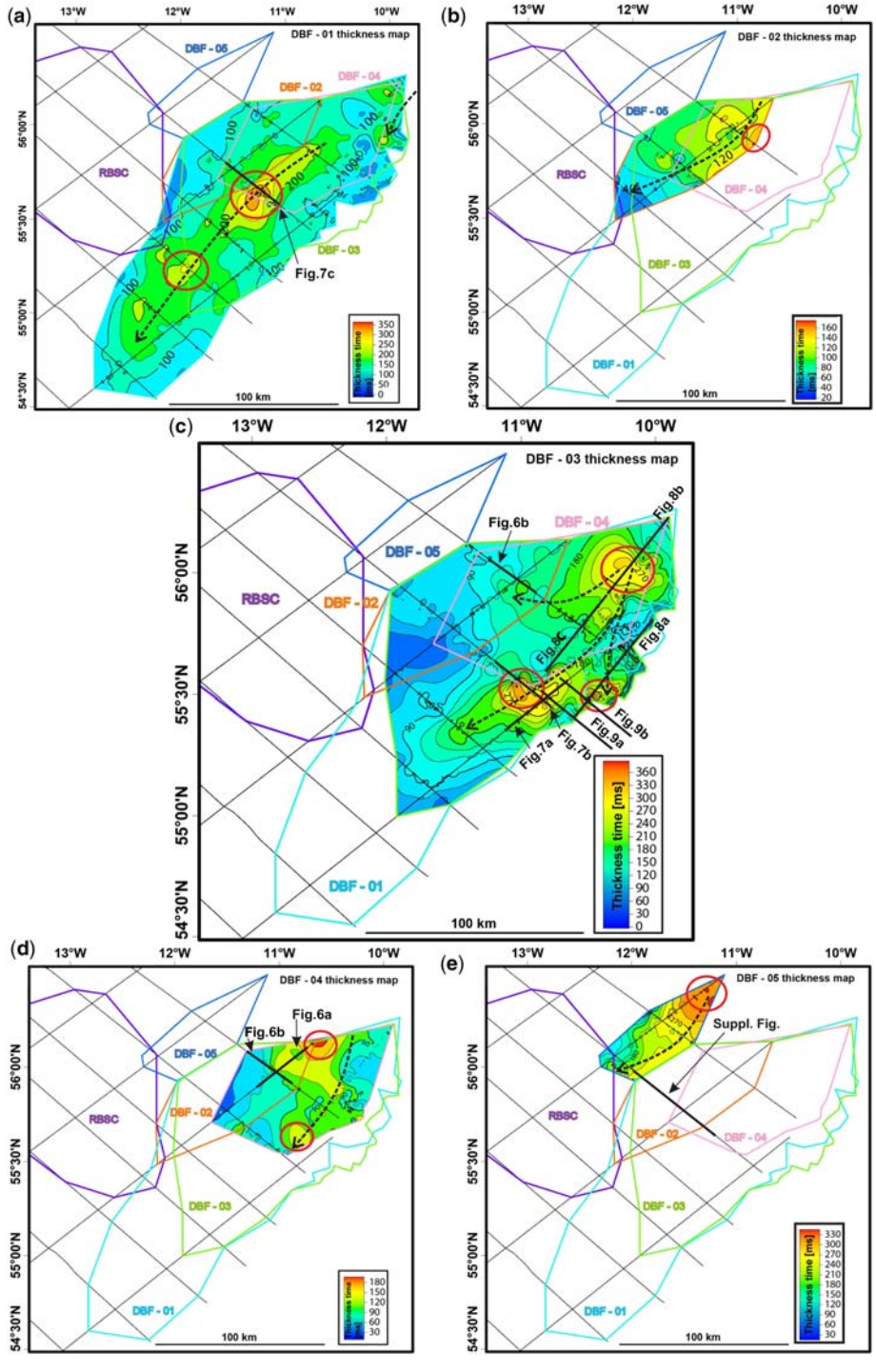

Fig. 5. (**a–e**) Thickness maps (TWT, ms) of different DBF complex MTDs, DBF 01–05. The extent of the RBSC shown in the above maps is the one mapped in this study. Depocentres are shown in red circles, dashed black lines represent flow direction of MTDs inferred from their respective thickness maps. 'Suppl. Fig.' indicates position of figure in Supplementary material.

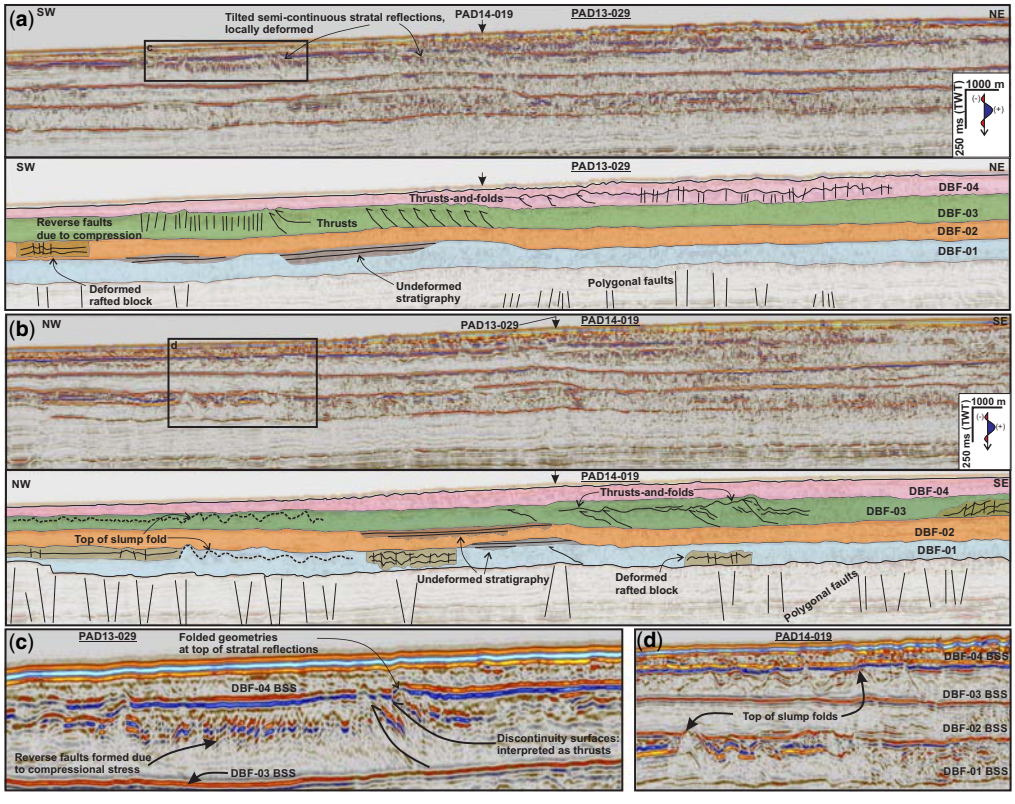

Fig. 6. (**a**, **b**) Multiple episodes of DBF in the NW part of study area. Compressional features such as thrust-and-folds within DBF-03 and DBF-04 are shown along with deformed rafted blocks within DBF-01 and DBF-02. Undeformed stratified sediments are interpreted between DBF-01 and DBF-02, and DBF-02 and DBF-03. (**c**, **d**) Zoom-in of compressional fold-and-thrust features in DBF-03, and top of slump folds in DBF-01 and DBF-03. Refer to Figure 5d for location of seismic sections.

of all the MTDs identified in this study (Fig. 10). The basal shear surface of DBF-02 is a continuous high-amplitude reflector, which separates it from the underlying DBF-01 unit (Fig. 6a, b). The maximum thickness of this slide is *c.* 180 ms (TWT), at a location where it meets the elevated morphology of DBF-01 (Fig. 5b). Most of the slide is draped by DBF-03, leaving *c.* 8–10% of the surface area covered by uniform stratified sediments (Fig. 4c). One minor deformed rafted block with a width of 5.5 km has been identified resting on the basal shear surface, within the thickest region of DBF-02. Undeformed stratigraphic units of stratified sediments have been identified in between DBF-01 and DBF-02 (Fig. 6a, b).

DBF-03

This MTD is 185 km long and 120 km wide in the central part of the slide, covering 65% of DBF-01 and most of DBF-02 (Fig. 2). It covers an area of 11 736 km^2 and comprises *c.* 1378 km^3 of sediments. The basal shear surface is a continuous high-amplitude reflector for most parts of the MTD (Figs 6a, b & 7a), with some exceptions of partially discontinuous, medium–high amplitude reflectors above some of the thrust-and-fold systems identified within DBF-03 (Fig. 7b). The discontinuous basal shear surface might be due to compressional deformation or some sort of seismic data processing artefacts. DBF-03 has the greatest thickness (*c.* 380 ms TWT) of all the MTDs identified in this study. Three depocentres have been identified (Fig. 5c). The southeastern depocentre is characterized by compressional features where it is found to be buttressed in a downslope position against the undisturbed sediments along the northeastern slope of the Rockall Trough (Fig. 9b). The southwestern depocentre is characterized by complex imbricate thrusts and compressional folding within the MTD (Fig. 7a, b). The flow direction of the MTD cannot be easily derived from the thrust

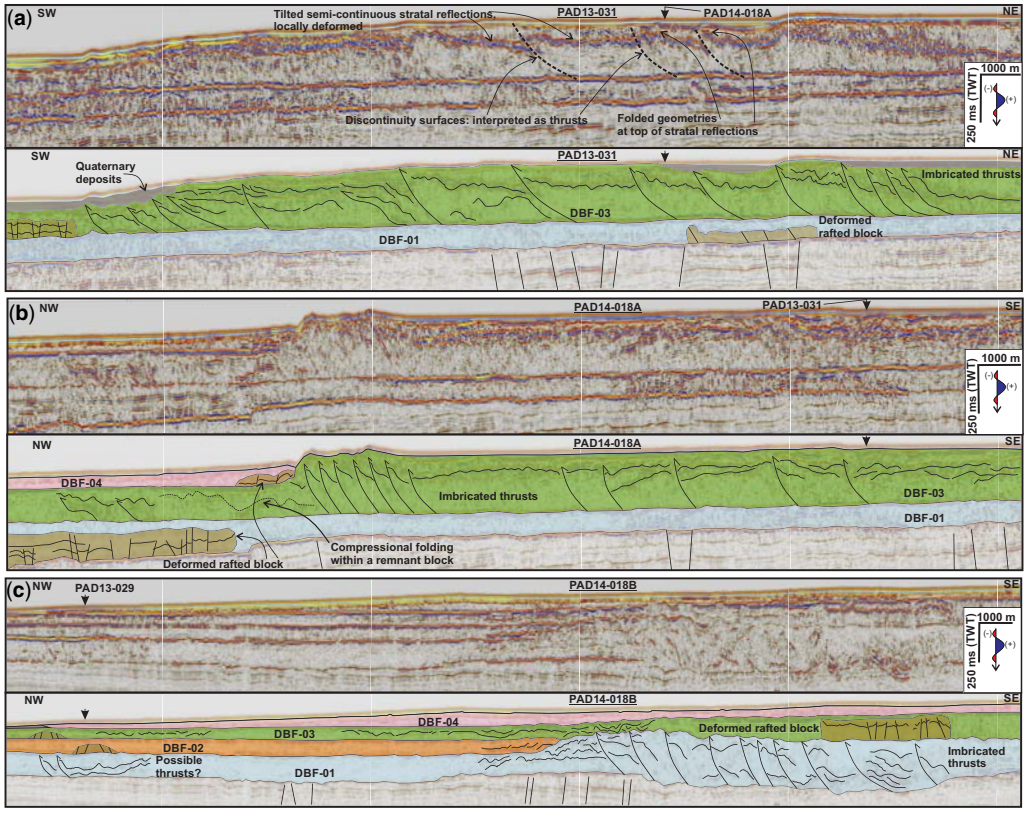

Fig. 7. (**a**–**c**) Fold-and-thrust and compressional folding structures within DBF-01, and DBF-03. Note the small-scale folded geometries at the tip of the stratal reflections, adjacent to the steeply-dipping discontinuities, which are interpreted as thrusts. Thrusts splay from the basal shear zone and steepen as it propagates upwards to the upper boundary of the MTD. Deformed rafted blocks are shown within DBF-01 and DBF-03. Refer to Figures 5a, c for location of seismic sections.

faults, which are identified using only two seismic lines, but this is discussed further later. The northernmost depocentre is characterized by compressional features formed over a 20 km long remnant block (Fig. 8b, c). Two other remnant blocks and 11 rafted deformed blocks have been identified within the DBF-03. More are expected to be present in between seismic lines. Their overall distribution is therefore not very well constrained; however, they are mostly observed in the central and northern part of the slide. Remnant blocks do not show any basal detachment, and hence represent isolated stationary blocks around which MTD material could have moved slowly. In contrast, rafted deformed blocks might have been subjected to faster-flowing MTD mass and have translated longer distances while being deformed at the same time (Bull *et al.* 2009).

DBF-04

This MTD is 118 km long and 80 km wide in the central part of the slide, covering almost 40% of DBF-03 (Fig. 2). It covers an area of 5036 km^2 and comprises of *c.* 378 km^3 of sediments. The basal shear surface is a continuous high-amplitude reflector for most parts of the MTD (Fig. 6a, b). It is partially discontinuous and characterized as a medium-high amplitude reflector in the southeastern part of the seismic section (Fig. 6b). The discontinuous nature of the basal shear surface is most likely due to the compressional features observed in these regions (Fig. 6a). However, there are regions of the MTD that are characterized by compressional features lying over a continuous high-amplitude basal shear surface. This variability in the imaging of the basal shear surface beneath the compressional

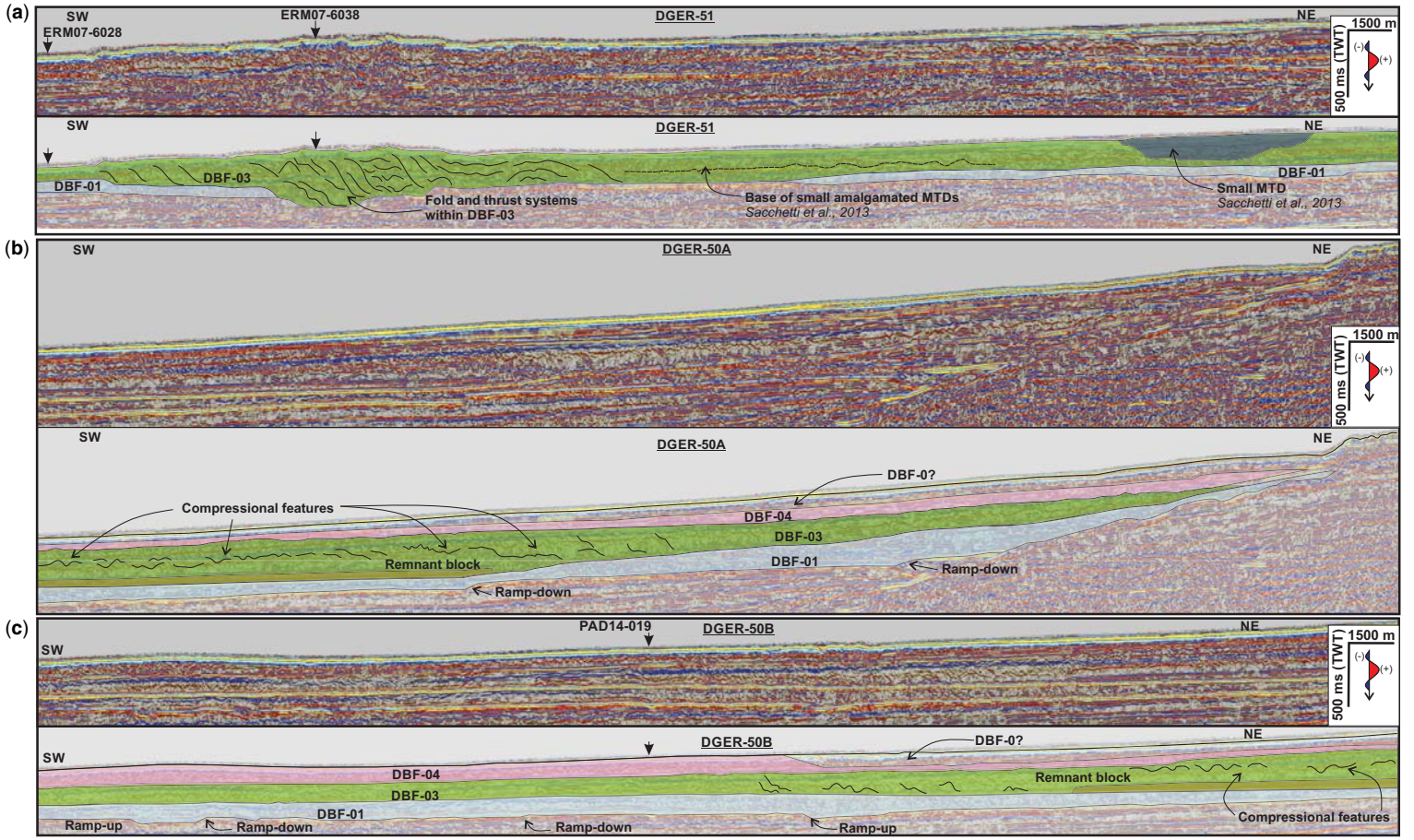

Fig. 8. (**a–c**) Downslope translation of DBF-01, DBF-03 and DBF-04, fold-and-thrusts within DBF-03 in the vicinity of a 20 km long remnant block. The basal shear surface is observed to ramp up and down the stratigraphy to create a series of staircase-like geometries, with clear reflection termination beneath the basal shear surface. Refer to Figure 5c for locations of seismic sections.

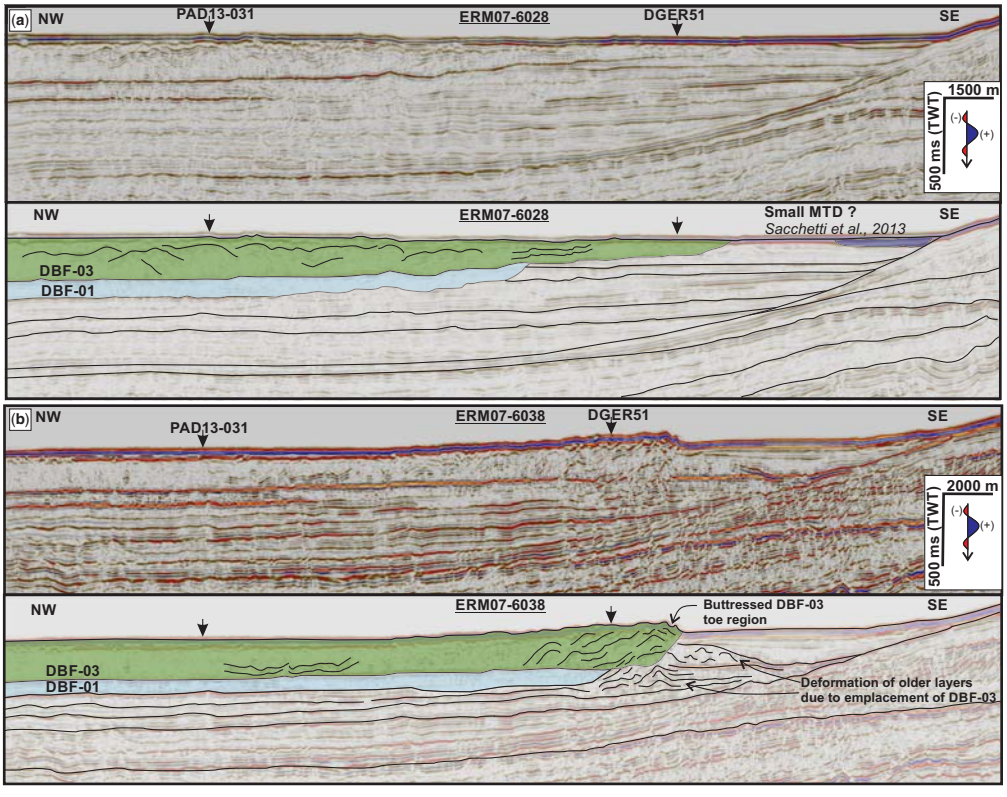

Fig. 9. (**a**) Compressional features within the toe region of the DBF-03, and a possible small MTD identified further SE in the seismic section, which overlaps with MTD interpretation of Sacchetti *et al.* (2013). (**b**) Development of compressional features where the toe region of DBF-03, which is found to be buttressed in a downslope position, is deforming parts of the strata (shown with minor folds). The basal shear surface of DBF-01 changes from high to low amplitude in both the figures; however the seismic facies inside the MTD is chaotic and easily distinguishable from the uniformly stratified underlying strata. Refer to Figure 5c for locations of seismic sections.

features could be related to the plasticity of sediments, degree of compression they have sustained or dewatering. DBF-04 has a maximum thickness of *c.* 200 ms TWT at the northern end of the slide (Fig. 5d). Considering the thickness distribution of the other deposits this implies that DBF-04 is substantially larger, and we are unable to image a large part of it due to lack of data coverage in that direction. However, a second depocentre of *c.* 150 ms TWT has been identified at the southern toe of the slide (Fig. 5d), which marks the region where DBF-04 is buttressed against the thrust faults of DBF-03 (Fig. 7b). A strongly deformed rafted block has also been identified at this meeting point of DBF-03 and DBF-04. Another 10.5 km long rafted block has been identified within this slide in the northern area where it is found to be thickest. This block is slightly-deformed as per the deformation styles illustrated by Gamboa *et al.* (2012). Thrust-reverse faults and compressional folding structures are observed only in the northern part of the slide (Fig. 6a, b).

DBF-05

This MTD is 91 km long and *c.* 34 km wide in the central part of the slide, not overlying or being overlain by any of the other MTDs. It covers an area of 1913 km^2 and comprises *c.* 384 km^3 of sediments. Even though it covers the smallest area out of all the MTDs, it does not have the smallest volume (Fig. 10). It attains a maximum thickness of *c.* 340 ms TWT in the northern part of the slide (Fig. 5e). Similar to DBF-04, the thickness distribution map suggests that a large part of the DBF-05 could not be imaged due to lack of data coverage in the north of the study area. The basal shear surface is a medium-high amplitude semi-continuous

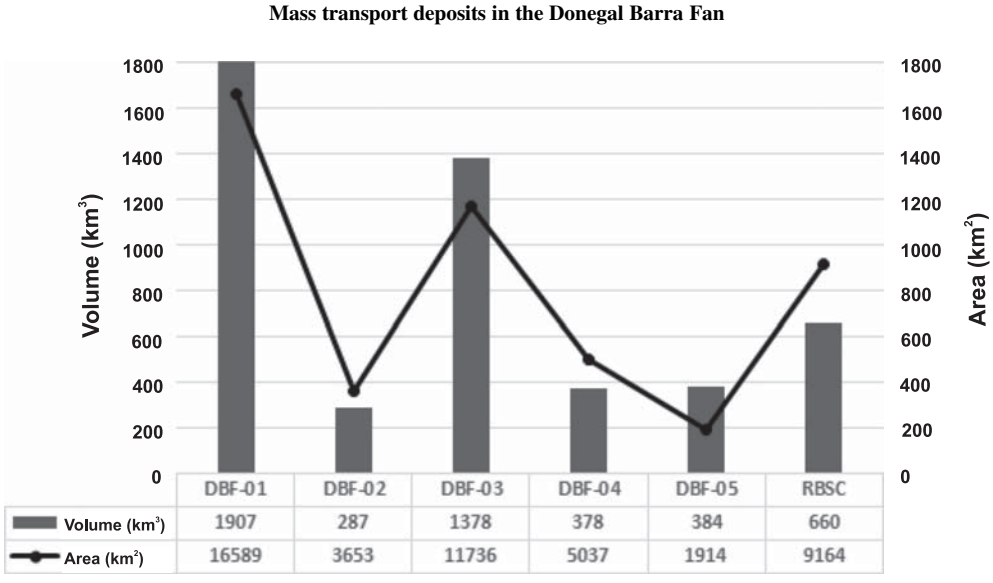

Fig. 10. Area and volume of the MTDs mapped in this study relating to the RBSC and DBF 01–05. Volume of each MTD was calculated by converting TWT into metres using an average P-wave velocity of 1700 m s^{-1} in less-consolidated marine sediments (Hamilton and Bachman 1982).

reflector in the northern part of the slide, and it gradually weakens in amplitude in the southern part. The contrasting difference between the chaotic semi–transparent facies of the MTD and the underlying evenly stratified undeformed layers assist in the interpretation of the basal shear surface (Fig. 3b). It has an impact on the underlying stratified layers and deforms them, as observed from the undulating reflections beneath the slide (Fig. 3a). This might have implications on the composition of sediments, water content and the fact that the DBF-05 toe is constrained by the pre-existing DBF-01, DBF-02 and DBF-03. DBF-05 is observed to truncate parts of DBF-01, DBF-02 and DBF-03 (Fig. 3a), which means that it postdates them. The toe of the RBSC forms a frontal ramp over the DBF-05 in the northwestern part of the study area, which suggests RBSC Slide C postdates DBF-05 (Fig. 3b).

Flow processes within DBF

The thickness distribution maps (Fig. 5a–e) allow us to consider how the morphology of each deposit affected the subsequent events. DBF-02 appears to occupy the northern area of DBF-01, which is where DBF-01 is the thinnest. DBF-03 appears to have ridden over the top of both of them, possibly because DBF-02 had smoothed out the topography to some degree. However, the fact that DBF-03's depocentre is off towards the base of slope, suggests that the DBF-02 deposit had probably raised the northern area enough to cause DBF-03 to be constrained to an area closer to the slope. DBF-04 is relatively small, relatively thin and expands over the top of DBF-03, suggesting that it might have been less viscous and more dilute. The depositional area of DBF-05 that differs from all the other four deposits suggests that DBF-01 to DBF-04 created a substantial relief on the seafloor, so that DBF-05 could no longer overcome the topography and had to flow around the Hebrides Terrace Seamount to occupy the lower relief in the basin, while still eroding the margins of the previous MTDs (Fig. 11). This pattern of compensational stacking is derived from the tendency deposits show to preferentially fill topographic lows, smoothing out topographic relief.

A group of semi-continuous stratal reflections are identified extending over *c.* 15–20 km on multiple seismic sections within DBF-01, DBF-03 and DBF-04 (Figs 6a, c & 7a). The stratal reflections are tilted (average: 5–10°) and locally deformed (Figs 6a & 7a). The tilted, deformed stratal reflections are observed to have an offset along surfaces (termed *discontinuities*) that dip more steeply than the dip angle of the stratal reflections (Figs 6c & 7a). Further, we also observe small-scale folded geometries at the tip of the stratal reflections, adjacent to the steeply dipping discontinuities (Figs 6c & 7a). These discontinuities seem to ramp up from the basal shear surface and steepen as they propagate upwards (Figs 6c, 7a & b). We interpret these discontinuity surfaces as thrust faults (Frey-Martínez *et al.* 2005; Bull *et al.* 2009). The maximum reverse throw of the thrusts is of the order 95 ms TWT, and an average of 40 ms TWT. Small thrusts terminate within the top of DBF-03

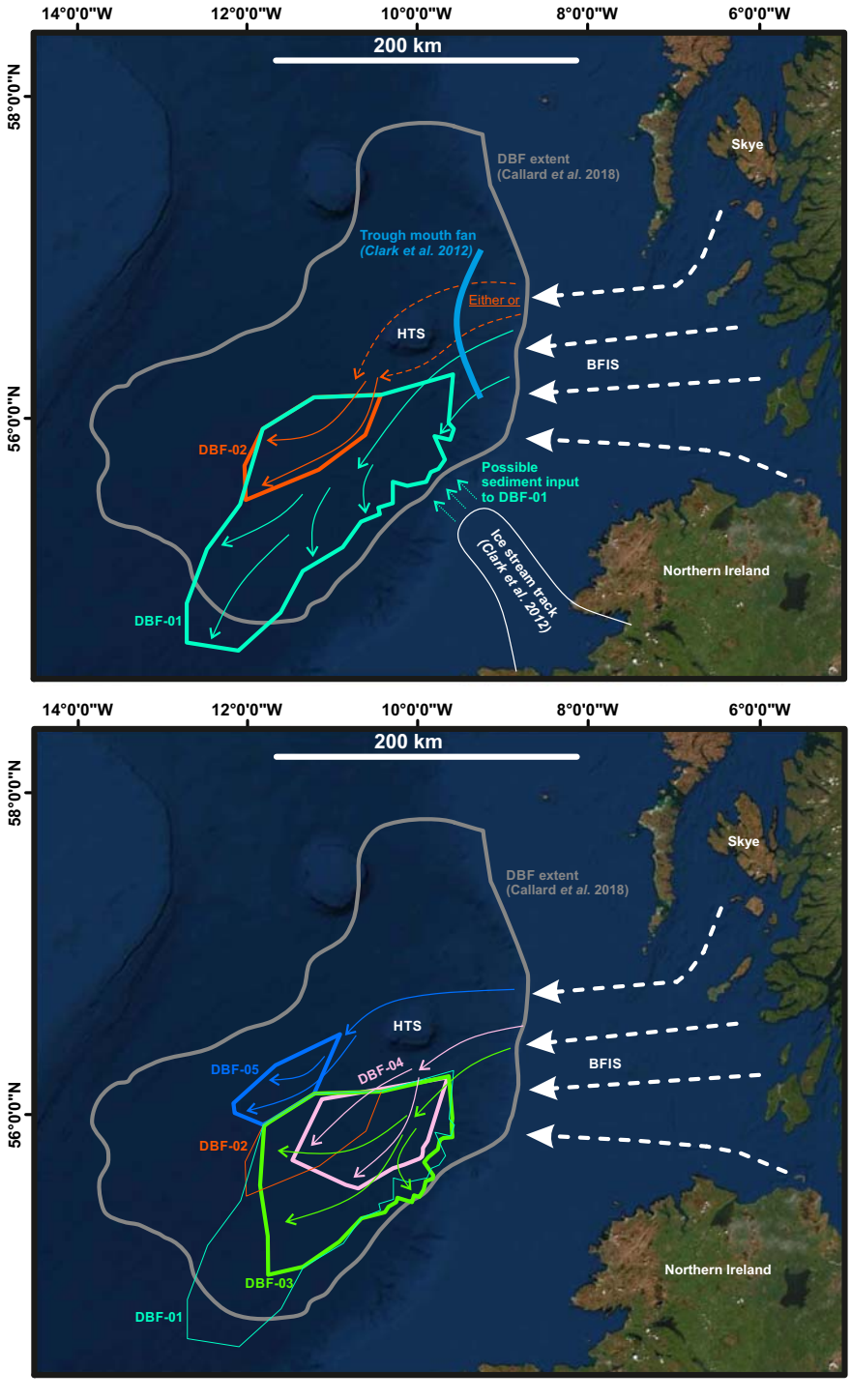

Fig. 11. Conceptual figure showing the Rockall Trough in NW Ireland and Barra Fan Ice Stream (BFIS) directions with estimate ages which have been responsible for the formation of the five MTDs identified within the Donegal Barra Fan (DBF) complex. Note the flow directions of each MTD slide (DBF 01–05), which have been derived from thickness maps and various types of kinematic indicators. HTS, Hebrides Terrace Seamount.

and DBF-04 (Fig. 6a, b). However, the largest thrust faults are observed to terminate at the upper boundary of the DBF-01 and DBF-03 (Fig. 7a, b & c). In general we do not observe any single thrust to emerge above the upper boundary of DBF-03, which is exposed to the seafloor (Fig. 7a, b). However, in the case of DBF-01, the upper tips of the thrusts were eroded in some instances by DBF-03 (Fig. 7c). Compressional folding structures and closely spaced reverse faults are typically observed basinward of the thrust faults in DBF-01 and DBF-03 (Figs 6 & 7b, c). Compressional folding structures are mostly observed above the remnant blocks (Fig. 8a). Usually compressional toe regions in submarine MTDs are dominated by thrusts-and-folds, which are classified as frontally confined MTDs (Frey-Martínez *et al.* 2006; Alsop *et al.* 2017). However, the MTDs of the DBF extend tens of kilometres beyond the regions dominated by thrusts-and-folds within the MTDs, implying that the MTDs still had mobility and were not fully arrested. This may infer the existence of a compressional regime within the MTD unrelated to arrest and freezing. This might also further suggest that the bulking up of the flow with the incorporation of extra material from the substrate changes the flow conditions locally to a more laminar, more plastic flow that causes a local velocity reduction and causes 'pile up' behind it. Similar examples have been described by Haughton *et al.* (2009). This may be similar to the processes that produce hybrid event beds, i.e. debrites encased in turbidites, resulting from rapid entrainment of mud-rich material from the substrate and/or rapid deceleration and vertical top-down flow transformation from turbidity current to debris flow which often lead to thickness increases in the deposits (e.g. Fonnesu *et al.* 2018; Pierce *et al.* 2018).

We observe thrust faults within DBF-01 on only one seismic line (Fig. 7c), within DBF-03 on five seismic lines separated by *c.* 55 km (Figs 6a, b, 7a, b & 8a), and within DBF-04 on only one seismic line (Fig. 6a). Frey-Martínez *et al.* (2006) derived flow directions of MTDs offshore Israel from the strike and dip directions of the thrust splays interpreted on high-resolution 3D seismic data. The actual strike and dip directions of the thrusts cannot be traced in each of the MTDs in this study; however, a general trend can be concluded from the contour lines on the thickness maps (Fig. 5). The NW-verging thrusts within DBF-01 (Fig. 7c) imply flow direction SE–NW. The BIIS ice stream flow lines from onshore Ireland had a similar flow direction (Fig. 11) (Clark *et al.* 2012). However, the contour lines corresponding to 200–350 ms TWT in the central part of the MTD (Fig. 5a) indicate a flow direction of NE–SW, which is more likely the general flow direction of the DBF complex. Thrusts in DBF-04 are observed in one single seismic line, dipping along the NE direction (Fig. 6a), which implies flow direction NE to SW. This aligns with the trend of contour lines corresponding to 90–150 ms TWT (Fig. 5d). Thrusts within the northern part of DBF-03 dip NE (Fig. 8a), which aligns with the general flow direction of the DBF complex and the contour lines observed. The trend of contour lines (120–270 ms TWT) of the thickness map in the northern part of DBF-03 implies two flow directions from the north (sediment source), i.e. north to SE and north to SW. However, in the southern part of DBF-03, two sets of seismic lines provide evidence of two different dip directions of the thrusts, i.e. SE and NE directions (Fig. 7a, b). There might be sediment input from the BIIS in the southern part of DBF-03, which will support the formation of NW-verging thrusts. However, given that we are only looking at one seismic line it might be that the thrusts are dipping in a direction anywhere within an arc between SE and NE, which is supported by the thickness map contour lines corresponding to 90–330 ms TWT in the southern part of DBF-03 (Fig. 5c). Moreover, if we consider that sediments of the MTD are flowing from SE to NW, then we do not expect to observe the buttressed toe of the MTD facing SE direction (Fig. 9b). Possible flow lines derived from a combined study of thrusts and thickness map contour lines are illustrated in Figures 5 and 11.

Susceptibility and triggering factors of MTDs

Various pre-conditioning factors such as sedimentation patterns, climatic history and tectonic events may influence a slope's susceptibility to failure, with slope failure events triggered by short-lived mechanisms such as earthquakes or destabilization of gas hydrates (Locat and Lee 2002; Masson *et al.* 2006).

Owen *et al.* (2007) observed a latitudinal trend in the occurrence of Late Pleistocene MTDs. In high-latitudes ($> 38°$ N), deglaciations increase sediment supply and seismicity related to isostatic uplift, hence increasing the likelihood of continental slope failures. The Pleistocene erosional glacial cycles associated with significant increase in sedimentation, along with the combined effect of continental uplift (Stoker *et al.* 2001), led to the development of MTDs along the northwestern European continental margin, including the DBF (Canals *et al.* 2004; Sultan *et al.* 2004*b*; Evans *et al.* 2005). The sediments were directly supplied from the BFIS and ice streams in Donegal Bay reflecting changes in ice sheet dynamics (Clark *et al.* 2012). In the North Sea Trough Mouth Fan, large-scale voluminous glaciogenic debrites coincide with and reflect periods when the ice sheet was at its maximum extent (King *et al.* 1998). We propose that the BFIS

oscillated between shelf edge and mid-shelf at least five times during the Pleistocene glaciations and that in those five times, it remained close enough to the shelf edge to deliver significant volumes of sediment that were then reworked downslope in the form of the five MTDs (DBF 01–05) documented in this study. This would suggest that the youngest of the events, DBF-05 corresponds to the Last Glacial Maximum (LGM), which is probably the last time the BFIS was at its maximum extent. This is corroborated by the fact that Slide C of RBSC ramps up over DBF-05 (Fig. 3b), and that Slide C of RBSC has been relatively accurately dated to be 21 ka (Georgiopoulou *et al.* 2019). It is difficult to assess the ages of the older DBF 01–04 events. They lie above the C10 unconformity, but we have demonstrated that there has been substantial erosion throughout the history of the DBF. Hence any inference about their ages is speculative without additional chronological data but can be attempted by correlation with what (little) is known about the BIIS dynamics in the Pleistocene. Most published records about the BIIS go back only to the LGM and some to Marine Isotope Stage (MIS) 5. Most of these records present counts of ice-rafted debris (IRD) over the last glacial periods. Peaks in IRD represent time of ice wasting rather than times of ice sheet maxima and maximum ice extent can be inferred to be from the time just preceding the peaks to the time of the largest peaks in the records (Scourse *et al.* 2009). Based on these published records, DBF-04 and DBF-05 could represent the latest ice advances on the shelf during the last glacial period, likely at some stage between 70 ka and 26 ka (Peck *et al.* 2007; Scourse *et al.* 2009; Hibbert *et al.* 2010). Another significant IRD peak in MIS6 (175–140 ka) might be related to the deposition of DBF-03 (Hibbert *et al.* 2010). Recent reconstructions suggest extensive glaciation during this time, known as the Penultimate Glacial Maximum (PGM), with a global sea-level lower than during the LGM (Rohling *et al.* 2017). Before the PGM, additional shelf-edge glaciations of Scottish ice are inferred during MIS 8 (300–243 ka) and MIS 10 (374–337 ka) with a first shelf- edge glaciation during MIS 12 (*c.* 0.45 Ma) based on a major seismic unconformity which is traced across the Hebrides shelf (Holmes *et al.* 2003; Sejrup *et al.* 2005). The resolution of the borehole records precludes unambiguous delineation between the age of IRD peaks between MIS 12 and MIS 8 (Sejrup *et al.* 2005), but it seems likely that the deposition of DBF-02 and DBF-01 took place as a result of these early episodes of glacial advances onto the shelf.

Indirect gas hydrate indicators as well as evidence of shallow gas and gas chimneys (fluid escape features) along the eastern slope of the Rockall Trough have been described recently (Minshull *et al.* 2020, fig. 9). Hydrates act as a cement between sediment grains and helps in binding them together (Clennell *et al.* 1999), but natural gas hydrates are very sensitive to changes in sea-bottom temperature and the pressure exerted by the water column above the seafloor (Ruppel and Kessler 2017). Any change of temperature and pressure could lead to the dissociation of gas hydrates which reduces the cohesive strength between sediment grains, and can lead to slope failures (Sultan *et al.* 2004*a*). Sedimentation pulses and increased sedimentation rates along glaciated margins can also trigger widespread gas hydrate dissociation (Karstens *et al.* 2018). The Gas Hydrate Stability Zone (GHSZ) thins down to 0–10 m along the eastern slope of the Rockall Trough (Minshull *et al.* 2020). It is possible that either fluid seepage or dissociation of hydrates along the slope, where the GHSZ is very sensitive to changes in pressure and temperature, could have triggered the MTDs in the Rockall Trough.

Conclusion

Interpretation of new high-resolution 2D multichannel seismic data in the northeastern part of the Rockall Trough of the Irish sector has produced a number of conclusions.

(1) Five episodes of mega-scale mass movements were identified in the Rockall Trough of the Irish sector, which are part of the DBF complex.
(2) The largest of the events, DBF-01, comprises *c.* 1907 km^3 of sediments, is the largest submarine MTD described in the NW British continental margin. A total volume of *c.* 5000 km^3 of sediments was mobilized by these five MTDs.
(3) Each of the MTDs may represent a time of BIIS maximum expansion. This would mean the BIIS reached maximum extent at least five times during the Pleistocene glaciations, and DBF-05 represents the LGM.
(4) The MTDs attained maximum thickness due to local deceleration and formation of fold-and-thrust zones several tens of kilometres before the MTD toe region.
(5) The slides show a compensational stacking pattern as the deposition of each MTD modifies the topography of the contemporaneous seafloor therefore influencing the position and transport direction of succeeding MTDs.

This study is an example of how improved understanding of the transport mechanisms and kinematic indicators of MTDs can be obtained from high-resolution 2D seismic data on continental margins. It also highlights that the investigation of MTDs

can improve understanding of long-term glacial histories.

Acknowledgements We are grateful for the valuable suggestions from two reviewers, Suzanne Bull and Uisdean Nicholson, and co-editor Davide Gamboa, who helped us to improve this paper. We acknowledge the Petroleum Affairs Division, Department of Communications, Climate Action & Environment, the Petroleum Infrastructure Programme, the Geological Survey Ireland and the Marine Institute (INFOMAR), for providing the data for this work. We also acknowledge Schlumberger for providing an academic license of Petrel software for this study.

Funding This publication derives from research supported in part by a research grant from Science Foundation Ireland (SFI) under Grant Number 13/RC/2092 and co-funded under the European Regional Development Fund and by iCRAG industry partners. SR also thanks the Irish Research Council Government of Ireland for the Postdoctoral Fellow Award Project No. GOIPD/2018/17).

Author contributions **SR**: conceptualization (equal), data curation (lead), formal analysis (lead), investigation (equal), methodology (lead), project administration (lead), visualization (lead), writing – original draft (lead), writing – review & editing (equal); **AG**: conceptualization (equal), formal analysis (supporting), investigation (equal), methodology (supporting), supervision (equal), validation (supporting), visualization (supporting), writing – review & editing (equal); **SB**: conceptualization (equal), formal analysis (supporting), supervision (equal), writing – review & editing (equal); **FS**: supervision (supporting), writing – review & editing (equal).

References

Alsop, G.I., Marco, S., Levi, T. and Weinberger, R. 2017. Fold and thrust systems in Mass Transport Deposits. *Journal of Structural Geology*, **94**, 98–115, https://doi.org/10.1016/j.jsg.2016.11.008

Armishaw, J.E., Holmes, R.W. and Stow, D.A.V. 2000. The Barra Fan: a bottom-current reworked, glacially-fed submarine fan system. *Marine and Petroleum Geology*, **17**, 219–238, https://doi.org/10.1016/S0264-8172(99)00049-5

Benetti, S., Dunlop, P. and Ó Cofaigh, C. 2010. Glacial and glacially-related features on the continental margin of northwest Ireland mapped from marine geophysical data. *Journal of Maps*, **6**, 14–29, https://doi.org/10.4113/jom.2010.1092

Bull, S., Cartwright, J. and Huuse, M. 2009. A review of kinematic indicators from mass-transport complexes using 3D seismic data. *Marine and Petroleum Geology*, **26**, 1132–1151, https://doi.org/10.1016/j.marpetgeo.2008.09.011

Callard, S.L., Ó Cofaigh, C. *et al*. 2018. Extent and retreat history of the Barra Fan Ice Stream offshore western Scotland and Northern Ireland during the last glaciation. *Quaternary Science Reviews*, **201**, 280–302, https://doi.org/10.1016/j.quascirev.2018.10.002

Canals, M., Lastras, G. *et al*. 2004. Slope failure dynamics and impacts from seafloor and shallow sub-seafloor geophysical data: case studies from the COSTA project. *Marine Geology*, **213**, 9–72, https://doi.org/10.1016/j.margeo.2004.10.001

Clark, C.D., Hughes, A.L.C., Greenwood, S.L., Jordan, C. and Sejrup, H.P. 2012. Pattern and timing of retreat of the last British–Irish Ice Sheet. *Quaternary Science Reviews*, **44**, 112–146, https://doi.org/10.1016/j.quascirev.2010.07.019

Clennell, M.B., Hovland, M., Booth, J.S., Henry, P. and Winters, W.J. 1999. Formation of natural gas hydrates in marine sediments: 1. Conceptual model of gas hydrate growth conditioned by host sediment properties. *Journal of Geophysical Research: Solid Earth (1978–2012)*, **104**, 22985–23003, https://doi.org/10.1029/1999JB900175

Dahlgren, K.I.T., Vorren, T.O., Stoker, M.S., Nielsen, T., Nygård, A. and Petter Sejrup, H. 2005. Late Cenozoic prograding wedges on the NW European continental margin: their formation and relationship to tectonics and climate. *Marine and Petroleum Geology*, **22**, 1089–1110, https://doi.org/10.1016/j.marpetgeo.2004.12.008

Dove, D., Arosio, R., Finlayson, A., Bradwell, T. and Howe, J.A. 2015. Submarine glacial landforms record Late Pleistocene ice-sheet dynamics, Inner Hebrides, Scotland. *Quaternary Science Reviews*, **123**, 76–90, https://doi.org/10.1016/j.quascirev.2015.06.012

Dowdeswell, J.A., Ó Cofaigh, C. *et al*. 2008. A major trough-mouth fan on the continental margin of the Bellingshausen Sea, West Antarctica: the Belgica Fan. *Marine Geology*, **252**, 129–140, https://doi.org/10.1016/j.margeo.2008.03.017

Dunlop, P., Shannon, R., McCabe, M., Quinn, R. and Doyle, E. 2010. Marine geophysical evidence for ice sheet extension and recession on the Malin Shelf: new evidence for the western limits of the British Irish Ice Sheet. *Marine Geology*, **276**, 86–99, https://doi.org/10.1016/j.margeo.2010.07.010

Elliott, G.M., Shannon, P.M., Haughton, P.D.W., Praeg, D. and O'Reilly, B. 2006. Mid- to Late Cenozoic canyon development on the eastern margin of the Rockall Trough, offshore Ireland. *Marine Geology*, **229**, 113–132, https://doi.org/10.1016/j.margeo.2006. 03.008

Elliott, G.M., Shannon, P.M., Haughton, P.D.W. and Ovrebo, L.K. 2010. The Rockall Bank Mass Flow: collapse of a moated contourite drift onlapping the eastern flank of Rockall Bank, west of Ireland. *Marine and Petroleum Geology*, **27**, 92–107, https://doi.org/10.1016/j.marpetgeo.2009.07.006

Evans, D., King, E.L., Kenyon, N.H., Brett, C. and Wallis, D. 1996. Evidence for long-term instability in the Storegga Slide region off western Norway. *Marine Geology*, **130**, 281–292, https://doi.org/10.1016/0025-3227(95)00135-2

Evans, D., Harrison, Z. *et al*. 2005. Palaeoslides and other mass failures of Pliocene to Pleistocene age along the Atlantic continental margin of NW Europe. *Marine and Petroleum Geology*, **22**, 1131–1148, https://doi.org/10.1016/j.marpetgeo.2005.01.010

Flood, R.D., Hollister, C.D. and Lonsdale, P. 1979. Disruption of the Feni sediment drift by debris flows from Rockall Bank. *Marine Geology*, **32**, 311–334, https://doi.org/10.1016/0025-3227(79)90070-7

Fonnesu, M., Felletti, F., Haughton, P.D.W., Patacci, M. and McCaffrey, W.D. 2018. Hybrid event bed character and distribution linked to turbidite system subenvironments: the North Apennine Gottero Sandstone (north-west Italy). *Sedimentology*, **65**, 151–190, https://doi.org/10.1111/sed.12376

Frey-Martínez, J., Cartwright, J. and Hall, B. 2005. 3D seismic interpretation of slump complexes: examples from the continental margin of Israel. *Basin Research*, **17**, 83–108, https://doi.org/10.1111/j.1365-2117.2005.00255.x

Frey-Martínez, J., Cartwright, J. and James, D. 2006. Frontally confined versus frontally emergent submarine landslides: a 3D seismic characterisation. *Marine and Petroleum Geology*, **23**, 585–604, https://doi.org/10.1016/j.marpetgeo.2006.04.002

Fyfe, J., Long, D., Evans, D. and Abraham, D.A. 1993. *The Geology of the Malin–Hebrides Sea Area*. HMSO for the British Geological Survey, London.

Gamboa, D., Alves, T. and Cartwright, J. 2011. Distribution and characterization of failed (mega)blocks along salt ridges, southeast Brazil: implications for vertical fluid flow on continental margins. *Journal of Geophysical Research: Solid Earth*, **116**, https://doi.org/10.1029/2011jb008357

Gamboa, D., Alves, T. and Cartwright, J. 2012. Seismic-scale rafted and remnant blocks over salt ridges in the Espírito Santo Basin, Brazil. *In*: Yamada, Y., Kawamura, K. *et al*. (eds) *Submarine Mass Movements and Their Consequences*. Advances in Natural and Technological Hazards Research, **31**. Springer, Dordrecht, 629–638.

Georgiopoulou, A., Benetti, S., Shannon, P.M., Haughton, P.D.W. and McCarron, S. 2012. Gravity flow deposits in the deep Rockall Trough, Northeast Atlantic. *In*: Yamada, Y., Kawamura, K. *et al*. (eds) *Submarine Mass Movements and Their Consequences*. Advances in Natural and Technological Hazards Research, **31**. Springer, Dordrecht, 695–707, https://doi.org/10.1007/978-94-007-2162-3_62

Georgiopoulou, A., Shannon, P.M., Sacchetti, F., Haughton, P.D.W. and Benetti, S. 2013. Basement-controlled multiple slope collapses, Rockall Bank Slide Complex, NE Atlantic. *Marine Geology*, **336**, 198–214, https://doi.org/10.1016/j.margeo.2012.12.003

Georgiopoulou, A., Benetti, S., Shannon, P.M., Sacchetti, F., Haughton, P.D.W., Comas-Bru, L. and Krastel, S. 2014. Comparison of mass wasting processes on the slopes of the Rockall Trough, Northeast Atlantic. *In*: Krastel, S., Behrmann, J.-H. *et al*. (eds) *Submarine Mass Movements and Their Consequences: 6th International Symposium*. Advances in Natural and Technological Hazards Research, **37**. Springer, 471–480.

Georgiopoulou, A., Krastel, S. *et al*. 2019. On the timing and nature of the multiple phases of slope instability on Eastern Rockall Bank, Northeast Atlantic. *Geochemistry, Geophysics, Geosystems*, **20**, 594–613, https://doi.org/10.1029/2018gc007674

Greenwood, S.L. and Clark, C.D. 2009. Reconstructing the last Irish Ice Sheet 2: a geomorphologically-driven model of ice sheet growth, retreat and dynamics. *Quaternary Science Reviews*, **28**, 3101–3123, https://doi.org/10.1016/j.quascirev.2009.09.014

Haflidason, H., Sejrup, H.P. *et al*. 2004. The Storegga Slide: architecture, geometry and slide development. *Marine Geology*, **213**, 201–234, https://doi.org/10.1016/j.margeo.2004.10.007

Hamilton, E.L. and Bachman, R.T. 1982. Sound velocity and related properties of marine sediments. *The Journal of the Acoustical Society of America*, **72**, 1891–1904, https://doi.org/10.1121/1.388539

Haughton, P., Davis, C., McCaffrey, W. and Barker, S. 2009. Hybrid sediment gravity flow deposits – Classification, origin and significance. *Marine and Petroleum Geology*, **26**, 1900–1918, https://doi.org/10.1016/j.marpetgeo.2009.02.012

Hibbert, F.D., Austin, W.E.N., Leng, M.J. and Gatliff, R.W. 2010. British Ice Sheet dynamics inferred from North Atlantic ice-rafted debris records spanning the last 175 000 years. *Journal of Quaternary Science*, **25**, 461–482, https://doi.org/10.1002/jqs.1331

Holmes, R., Long, D. and Dodd, L.R. 1998. Large-scale debrites and submarine landslides on the Barra Fan, west of Britain. *Geological Society, London, Special Publications*, **129**, 67–79, https://doi.org/10.1144/gsl.Sp.1998.129.01.05

Holmes, R., Bulat, J., Hamilton, I. and Long, D. 2003. Morphology of an ice-sheet limit and constructional glacially-fed slope front, Faroe–Shetland Channel. *In*: Mienert, J. and Weaver, P. (eds) *European Margin Sediment Dynamics: Side-Scan Sonar and Seismic Images*. Springer, Berlin, 149–152.

Huvenne, V.A.I., Croker, P.F. and Henriet, J.-P. 2002. A refreshing 3D view of an ancient sediment collapse and slope failure. *Terra Nova*, **14**, 33–40, https://doi.org/10.1046/j.1365-3121.2002.00386.x

Karstens, J., Haflidason, H. *et al*. 2018. Glacigenic sedimentation pulses triggered post-glacial gas hydrate dissociation. *Nature Communications*, **9**, 635, https://doi.org/10.1038/s41467-018-03043-z

King, E.L., Haflidason, H., Sejrup, H.P. and Løvlie, R. 1998. Glacigenic debris flows on the North Sea Trough Mouth Fan during ice stream maxima. *Marine Geology*, **152**, 217–246, https://doi.org/10.1016/S0025-3227(98)00072-3

Knutz, P.C., Austin, W.E.N. and Jones, E.J.W. 2001. Millennial-scale depositional cycles related to British Ice Sheet variability and North Atlantic paleocirculation since 45 kyr B.P., Barra Fan, U.K. margin. *Paleoceanography*, **16**, 53–64, https://doi.org/10.1029/1999pa000483

Knutz, P.C., Jones, E.J.W., Howe, J.E., Van Weering, T.J.C. and Stow, D.A.V. 2002. Wave-form sheeted contourite drift on the Barra Fan, NW UK continental margin. *Geological Society, London, Memoirs*, **22**, 85–97, https://doi.org/10.1144/gsl.Mem.2002.022.01.08

Locat, J. and Lee, H.J. 2002. Submarine landslides: advances and challenges. *Canadian Geotechnical Journal*, **39**, 193–212, https://doi.org/10.1139/t01-089

Maslin, M., Owen, M., Day, S. and Long, D. 2004. Linking continental-slope failures and climate change: testing the clathrate gun hypothesis. *Geology*, **32**, 53–56, https://doi.org/10.1130/G20114.1

Masson, D.G., Harbitz, C.B., Wynn, R.B., Pedersen, G. and Løvholt, F. 2006. Submarine landslides: processes, triggers and hazard prediction. *Philosophical Transactions of the Royal Society A: Mathematical, Physical and Engineering Sciences*, **364**, 2009–2039, https://doi.org/10.1098/rsta.2006.1810

McDonnell, A. and Shannon, P.M. 2001. Comparative Tertiary stratigraphic evolution of the Porcupine and Rockall basins. *Geological Society, London, Special Publications*, **188**, 323–344, https://doi.org/10.1144/gsl.sp.2001.188.01.19

Minshull, T.A., Marín-Moreno, H. *et al*. 2020. Hydrate occurrence in Europe: a review of available evidence. *Marine and Petroleum Geology*, **111**, 735–764, https://doi.org/10.1016/j.marpetgeo.2019.08.014

Moscardelli, L. and Wood, L. 2016. Morphometry of mass-transport deposits as a predictive tool. *GSA Bulletin*, **128**, 47–80, https://doi.org/10.1130/b31221.1

Ó Cofaigh, C., Taylor, J., Dowdeswell, J.A. and Pudsey, C.J. 2003. Palaeo-ice streams, trough mouth fans and high-latitude continental slope sedimentation. *Boreas*, **32**, 37–55, https://doi.org/10.1080/0300948031000 1858

Ó Cofaigh, C., Dunlop, P. and Benetti, S. 2012. Marine geophysical evidence for Late Pleistocene ice sheet extent and recession off northwest Ireland. *Quaternary Science Reviews*, **44**, 147–159, https://doi.org/10.1016/j.quascirev.2010.02.005

Ó Cofaigh, C., Weilbach, K. *et al*. 2019. Early deglaciation of the British-Irish Ice Sheet on the Atlantic shelf northwest of Ireland driven by glacioisostatic depression and high relative sea level. *Quaternary Science Reviews*, **208**, 76–96, https://doi.org/10.1016/j.quascirev.2018.12.022

Owen, M.J. and Long, D. 2016. Barra Fan: a major glacial depocentre on the western continental margin of the British Isles. *Geological Society, London, Memoirs*, **46**, 359, https://doi.org/10.1144/M46.76

Owen, M., Day, S. and Maslin, M. 2007. Late Pleistocene submarine mass movements: occurrence and causes. *Quaternary Science Reviews*, **26**, 958–978, https://doi.org/10.1016/j.quascirev.2006.12.011

Owen, M.J., Maslin, M.A., Day, S.J. and Long, D. 2018. Sediment failures within the Peach Slide (Barra Fan, NE Atlantic Ocean) and relation to the history of the British-Irish Ice Sheet. *Quaternary Science Reviews*, **187**, 1–30, https://doi.org/10.1016/j.quascirev.2018.03.018

Peck, V.L., Hall, I.R., Zahn, R. and Scourse, J.D. 2007. Progressive reduction in NE Atlantic intermediate water ventilation prior to Heinrich events: response to NW European ice sheet instabilities? *Geochemistry, Geophysics, Geosystems*, **8**, https://doi.org/10.1029/2006gc001321

Peters, J.L., Benetti, S., Dunlop, P. and Ó Cofaigh, C. 2015. Maximum extent and dynamic behaviour of the last British–Irish Ice Sheet west of Ireland. *Quaternary Science Reviews*, **128**, 48–68, https://doi.org/10.1016/j.quascirev.2015.09.015

Peters, J.L., Benetti, S., Dunlop, P., Ó Cofaigh, C., Moreton, S.G., Wheeler, A.J. and Clark, C.D. 2016. Sedimentology and chronology of the advance and retreat of the last British-Irish Ice Sheet on the continental shelf west of Ireland. *Quaternary Science Reviews*, **140**, 101–124, https://doi.org/10.1016/j.quascirev.2016.03.012

Pierce, C.S., Haughton, P.D.W., Shannon, P.M., Pulham, A.J., Barker, S.P. and Martinsen, O.J. 2018. Variable character and diverse origin of hybrid event beds in a sandy submarine fan system, Pennsylvanian Ross Sandstone Formation, western Ireland. *Sedimentology*, **65**, 952–992, https://doi.org/10.1111/sed.12412

Rebesco, M., Camerlenghi, A., Geletti, R. and Canals, M. 2006. Margin architecture reveals the transition to the modern Antarctic ice sheet ca. 3 Ma. *Geology*, **34**, 301–304, https://doi.org/10.1130/g22000.1

Rohling, E.J., Hibbert, F.D. *et al*. 2017. Differences between the last two glacial maxima and implications for ice-sheet, δ18O, and sea-level reconstructions. *Quaternary Science Reviews*, **176**, 1–28, https://doi.org/10.1016/j.quascirev.2017.09.009

Ruppel, C.D. and Kessler, J.D. 2017. The interaction of climate change and methane hydrates. *Reviews of Geophysics*, **55**, 126–168, https://doi.org/10.1002/2016RG000534

Sacchetti, F., Benetti, S., Georgiopoulou, A., Dunlop, P. and Quinn, R. 2011. Geomorphology of the Irish Rockall Trough, North Atlantic Ocean, mapped from multibeam bathymetric and backscatter data. *Journal of Maps*, **7**, 60–81, https://doi.org/10.4113/jom.2011.1157

Sacchetti, F., Benetti, S. *et al*. 2012. Deep-water geomorphology of the glaciated Irish margin from high-resolution marine geophysical data. *Marine Geology*, **291-294**, 113–131, https://doi.org/10.1016/j.margeo.2011.11.011

Sacchetti, F., Benetti, S., Quinn, R. and Ó Cofaigh, C. 2013. Glacial and post-glacial sedimentary processes in the Irish Rockall Trough from an integrated acoustic analysis of near-seabed sediments. *Geo-Marine Letters*, **33**, 49–66, https://doi.org/10.1007/s00367-012-0310-2

Salmanidou, D., Georgiopoulou, A., Guillas, S. and Dias, F. 2018. Rheological considerations for the modelling of submarine sliding at Rockall Bank, NE Atlantic Ocean. *Physics of Fluids*, **30**, 030705, https://doi.org/10.1063/1.5009552

Scourse, J.D., Haapaniemi, A.I. *et al*. 2009. Growth, dynamics and deglaciation of the last British–Irish ice sheet: the deep-sea ice-rafted detritus record. *Quaternary Science Reviews*, **28**, 3066–3084, https://doi.org/10.1016/j.quascirev.2009.08.009

Sejrup, H.P., Hjelstuen, B.O. *et al*. 2005. Pleistocene glacial history of the NW European continental margin. *Marine and Petroleum Geology*, **22**, 1111–1129, https://doi.org/10.1016/j.marpetgeo.2004.09.007

Shannon, P.M., O'Reilly, B.M., Readman, P.W., Jacob, A.W.B. and Kenyon, N. 2001. Slope failure features on the margins of the Rockall Trough. *Geological Society, London, Special Publications*, **188**, 455–464, https://doi.org/10.1144/gsl.sp.2001.188.01.28

Stoker, M.S., Van Weering, T.C.E. and Svaerdborg, T. 2001. A Mid- to Late Cenozoic tectonostratigraphic framework for the Rockall Trough. *Geological Society, London, Special Publications*, **188**, 411–438, https://doi.org/10.1144/gsl.sp.2001.188.01.26

Stow, D.A.V., Armishaw, J.E. and Holmes, R. 2002. Holocene contourite sand sheet on the Barra Fan slope, NW Hebridean margin. *Geological Society, London, Memoirs*, **22**, 99, https://doi.org/10.1144/GSL.MEM.2002.022.01.09

Sultan, N., Cochonat, P., Foucher, J.P. and Mienert, J. 2004*a*. Effect of gas hydrates melting on seafloor slope instability. *Marine Geology*, **213**, 379–401, https://doi.org/10.1016/j.margeo.2004.10.015

Sultan, N., Cochonat, P. *et al*. 2004*b*. Triggering mechanisms of slope instability processes and sediment failures on continental margins: a geotechnical approach. *Marine Geology*, **213**, 291–321, https://doi.org/10.1016/j.margeo.2004.10.011

Tarlati, S. 2018. *Late Quaternary reconstruction of British-Irish Ice Sheet variability through the analysis of deep-water sediments from the Donegal Barra Fan and the Rockall Trough, North Atlantic*. PhD thesis, Ulster University.

Unnithan, V., Shannon, P.M., McGrane, K., Readman, P.W., Jacob, A.W.B., Keary, R. and Kenyon, N.H. 2001. Slope instability and sediment redistribution in the Rockall Trough: constraints from GLORIA. *Geological Society, London, Special Publications*, **188**, 439–454, https://doi.org/10.1144/gsl.sp.2001.188.01.27

Varnes, D.J. 1978. Slope movement types and processes. *TRB Special Report*, **176**, 11–33.

Vorren, T.O. and Laberg, J.S. 1997. Trough mouth fans – palaeoclimate and ice-sheet monitors. *Quaternary Science Reviews*, **16**, 865–881, https://doi.org/10.1016/S0277-3791(97)00003-6

Yilmaz, Ö. 2001. *Seismic Data Analysis: Processing, Inversion, and Interpretation of Seismic Data*. Society of Exploration Geophysicists, Tulsa.